Steel and Composite Structures, Vol. 1, No. 2 (2001) 231-244
DOI: http://dx.doi.org/10.12989/scs.2001.1.2.231

FRP or steel plate-to-concrete bonded joints: Effect of test methods on experimental bond strength

J.F. Chen†

School of the Built Environment, Nottingham University, University Park, Nottingham NG7 2RD, U.K.

Z.J. Yang‡ and G.D. Holt‡†

Built Environment Research Unit, School of Engineering and the Built Environment, Wolverhampton University, Wolverhampton WV1 1SB, U.K.

Abstract. The strengthening of reinforced concrete structures using externally bonded steel or advanced fibre reinforced plastic (FRP) composites is becoming increasingly common. A key factor affecting the behaviour and reliability of such strengthened structures is the bond strength between the steel or FRP plate and the concrete substrate. Several different experimental set-ups have previously been used to determine bond strength. This paper presents a careful finite element analysis of the stress distributions in these test set-ups. Results show that stress distributions can be significantly different for different set-ups, for similar materials and geometry.

Key words: bond strength; bond test; concrete; finite element method; FRP; shear test; steel plate; strengthening; test method.

1. Introduction

Strengthening of reinforced concrete (RC) structures using externally bonded steel or advanced fibre reinforced plastic (FRP) composites is being increasingly used. One of the major factors affecting the behaviour of such strengthened structures is the bond strength between the reinforcement plate and the concrete substrate. Recent studies have shown that a comprehensive understanding of the bond behaviour is essential in predicting various de-bonding failure modes such as intermediate crack induced debonding in flexurally strengthened beams and slabs (Teng *et al.* 2000, Smith *et al.* 2001), and debonding of side plates in shear strengthened beams (Chen and Teng 2001a). The accurate determination of bond strength is therefore essential for safe design of strengthening schemes for RC structures using externally bonded plates.

There is presently a lack of standards concerning the test methods for determining the bond strength. Several different experimental set-ups, including various shear tests and modified beam tests have been used. Although substantial research has been carried out on understanding bond strength (see Chen and Teng 2001b), Horiguchi and Saeki (1997) appear to have been the first to have experimentally

†Lecturer in Structural Engineering
‡Research Student
‡†Reader in Construction Management

investigated the effect of different test methods on test results. They concluded that different test set-ups have a significant effect on the resultant test bond strength. This paper first presents a review of different test methods. A finite element (FE) study on the stress distributions in these set-ups is then carried out. A comparison is made to investigate the difference between the different test methods.

Based on an extensive literature review, Chen and Teng (2001b) indicated that most bond strength test specimens failed a few millimetres in the concrete underneath the concrete/ adhesive interface. In this failure mode, a good bond strength model should be applicable to both FRP and steel plate bonded to concrete (e.g., Chen and Teng 2001b). No distinction is therefore made between FRP and steel plates in this paper.

2. Bond strength test methods

2.1. Classification

Bond strength between FRP or steel plates and concrete blocks has commonly been tested using a shear test or modified beam test. According to the differences in mechanical behaviour, the test set-ups can be classified as: a) double shear pulling (DoublePull) test; b) double shear pushing (DoublePush) test; c) single shear pulling (SinglePull) test; d) single shear pushing (SinglePush) test; and e) beam (or bending) test (BeamTest).

It may be noted that numerous studies have been performed on flexurally strengthened beams. Some of these were concerned with the anchorage length of externally bonded plates (e.g., Jones *et al.* 1980, Garden *et al.* 1998). These belong to the "true beam bending" test and the results cannot be easily related to bond strength as applicable to this paper. They are thus beyond the remit of the present discussion.

2.2. Double shear pulling (DoublePull) test

The DoublePull test has been the most popular test method to date (e.g., van Gemert 1980, Kobatake *et al.* 1993, Autocon 1994, Brosens and van Gemert 1997, Hiroyuki and Wu 1997, Fukuzawa *et al.* 1997, Maeda *et al.* 1997). There are slight differences regarding the test set-up details, but the loading mechanism is similar (Fig. 1a). Two test plates are bonded on opposing sides of a concrete block and equal tensile forces P_p are applied in the plates. These forces are balanced by a pulling force applied in the concrete P_c which may be applied either through a steel bar embedded at the centre of the concrete block, or through steel plates bonded on the sides of the concrete block.

2.3. Double shear pushing (DoublePush) test

The pushing force acting on the concrete block in a DoublePush test (Fig. 1b) is usually applied through a supporting wedge (e.g., Swamy *et al.* 1986, Neubauer and Rostásy 1997). The latter believed that this can simulate well the stress state in the anchorage zone of a flexurally strengthened beam. Obviously, the stresses in the loading direction are compressive in the concrete block in this set-up; whilst the corresponding stresses in a DoublePull test are tensile. This difference may lead to discrepancies among test results.

2.4. Single shear pulling (SinglePull) test

Although no studies appear to have used such a test set-up, theoretically a SinglePull test could be

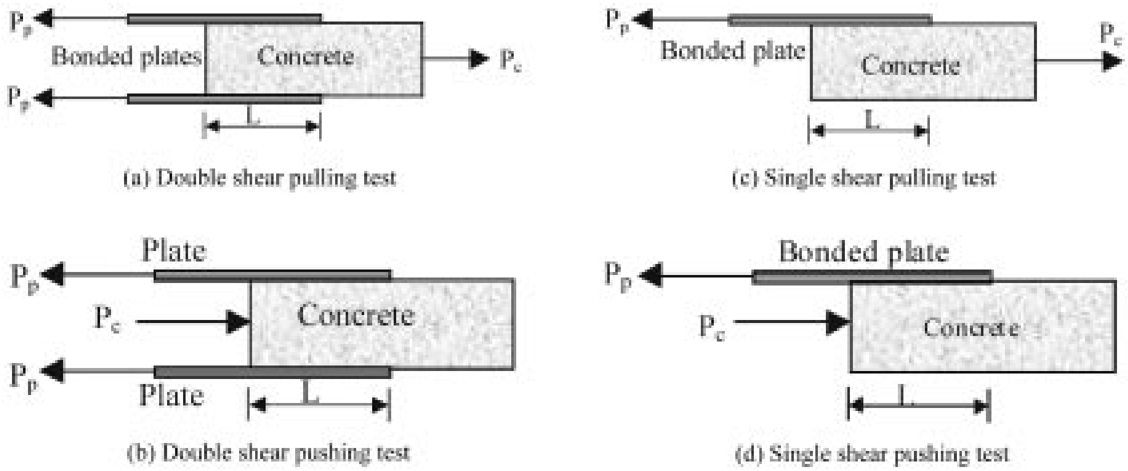

Fig. 1 Shear test schemes

used (Fig. 1c). Here, only one plate would be bonded onto one side of the concrete block. This leads to a loss of symmetry (as exists in a DoublePull test).

2.5. Single shear pushing (SinglePush) test

The SinglePush test (Fig. 1d) has possibly been the second most popular set-up after the DoublePull test (e.g., Chajes *et al.* 1996, Täljsten 1997, Bizindavyi and Neale 1999). This can obviously offer savings in both materials and labour because only one plate coupon is bonded to the concrete.

However, the stress state in the concrete in this test method can be expected to be quite different from that in the double shear pulling test. Therefore, significant difference may exist between these two methods.

2.6. Beam (or Bending) test (BeamTest)

The BeamTest can well simulate the effects of moment variation and shear force in the concrete block. Similar test set-ups were adopted by van Gemert (1980) to investigate steel-concrete anchorage behaviour (Fig. 2a) and Ziraba *et al.* (1995) to investigate the effect of concrete compressive strength on steel-concrete bond strength (Fig. 2b). The latter found no dependence of the failure of the joint to the concrete strength and concluded that the concrete-glue-plate interface behaviour was rather a surface phenomenon. However, this contradicts other experimental observations that concrete strength does have significant effect on bond strength (e.g., Chajes *et al.* 1996, Horiguchi and Saeki 1997).

3. Finite element modelling

3.1. Modelling

Linear elastic FE analyses were carried out in this study to compare the stress states in different test

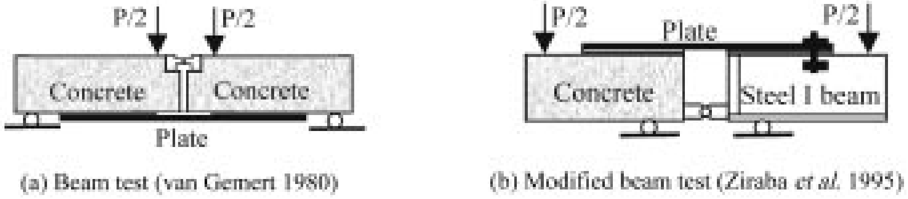

Fig. 2 Beam tests

schemes. The concrete block was taken to have a size of 500 mm in length and 150 mm in thickness so that various bond lengths (of the plate to the block) could be analysed without changing the blocks dimensions. A plate thickness of 3 mm and adhesive thickness of 1 mm were assumed in all of the analyses. Young's modulus was assumed to be 200, 1 and 30 GPa for the plate, adhesive and concrete respectively. The corresponding Poisson's ratio was 0.3, 0.25 and 0.17 respectively. The geometry, the loading and boundary conditions, as assumed for all five test schemes, were taken to be as shown in Fig. 3. For symmetrical configurations, only half of the structure was modelled. The pulling force in the plate was applied by a uniformly distributed tension force q with an intensity of 55.55 MPa (equivalent to applying 10 kN on a 3×60 mm plate) at the loading end for shear tests. The point load P applied in the modified beam test was obtained based on static equilibrium by assuming the same stress value in the plate.

The analyses were conducted using an FE analysis package which is being specially developed for analysing the behaviour of RC structures strengthened with externally bonded plates using a fracture mechanics approach. All materials were modelled using 8-node quadrilateral isoparametric plane stress elements. A perfect bond between the adhesive and the plate and between the adhesive and the concrete was assumed.

3.2. Mesh convergence test

A mesh convergence test was conducted for the double shear pulling test (bond length L =100 mm). Results from four typical meshes are compared here. All meshes have 8 layers of elements for the plate and 30 layers of elements for the concrete block in the vertical direction. For brevity, the left end of the adhesive where the plate is loaded is referred to as the "pull end" whilst the right end of the adhesive where the plate ends is referred to as the "plate end". Meshes were finest near the pull and the plate ends, where stress singularities exist (Fig. 4a). They gradually became coarser towards other parts of the structure. The numbers of element layers used for the adhesive layer for these four meshes were 2, 4, 10 and 20 respectively. Corresponding smallest element sizes for them were 0.5, 0.25, 0.1, and 0.05 mm respectively. Fig. 4a shows the mesh with the smallest element size being 0.1 mm. Mesh details around the pull and the plate end are shown in Figs. 4b and 4c respectively. For brevity, the plate-adhesive interface, adhesive-concrete interface and the mid-section of adhesive (Fig. 4) are respectively referred to as PA, AC and AM hereafter.

Figs. 5a and 5b show distributions of the normal interfacial stress σ_y (or peeling stress) at PA near the pull and plate ends respectively. Maximum stresses near the ends increase as the mesh becomes finer. This is due to stress singularities at two-material wedges (Hein and Erdogan 1971). There are four stress singular points in this problem (Points A, C, D and F in Figs. 4b and c). The normal stress is compressive at PA but tensile at AC near the plate end, which is similar to the stress distribution near the plate end in a RC beam bonded with a soffit plate as investigated by Teng *et al.* (2001). The normal

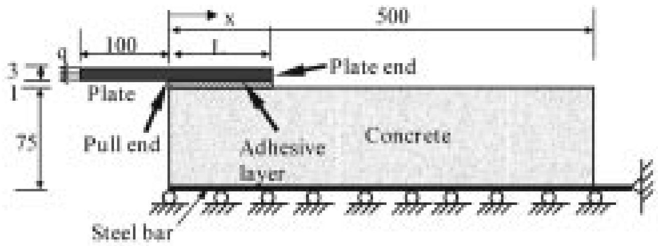

(a) Double shear pulling test

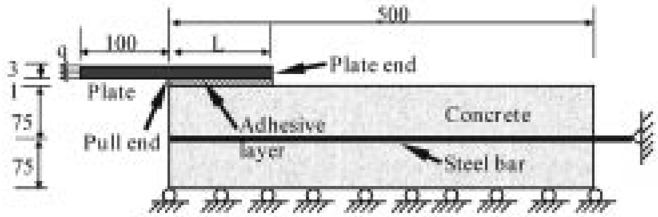

(b) Single shear pulling test

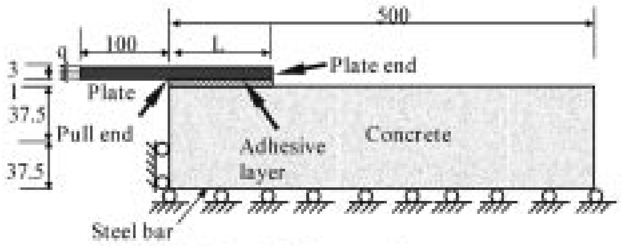

(c) Double shear push test

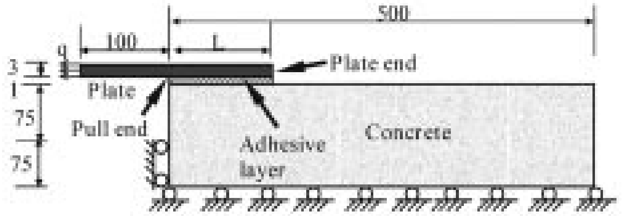

(d) Single shear pulling test

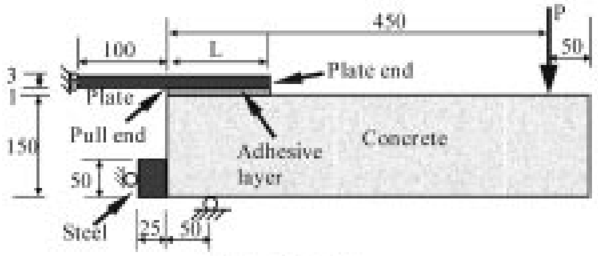

(e) Modified beam test

Fig. 3 Geometry and boundary conditions for FE modelling

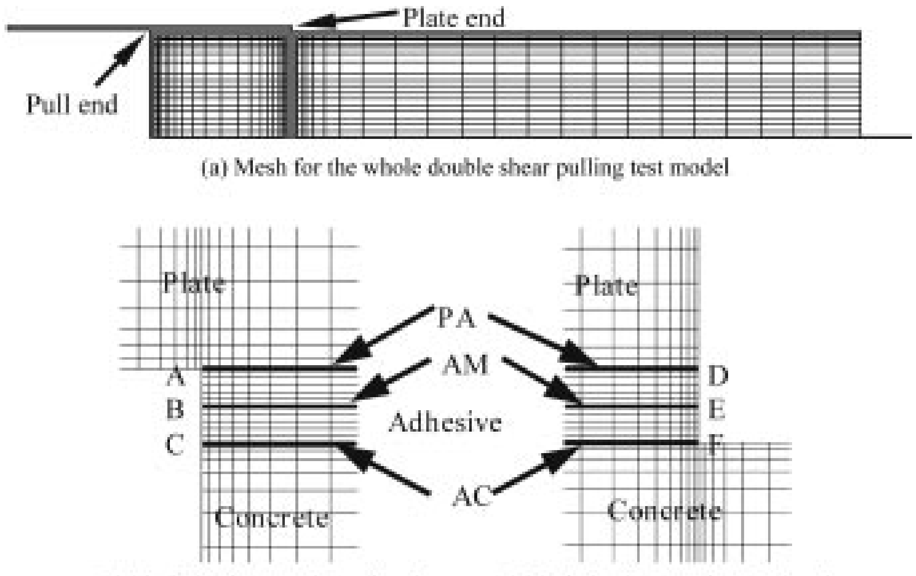

(a) Mesh for the whole double shear pulling test model

(b) Mesh details near the pull end (c) Mesh details near the platel end

Fig. 4 A typical FE mesh

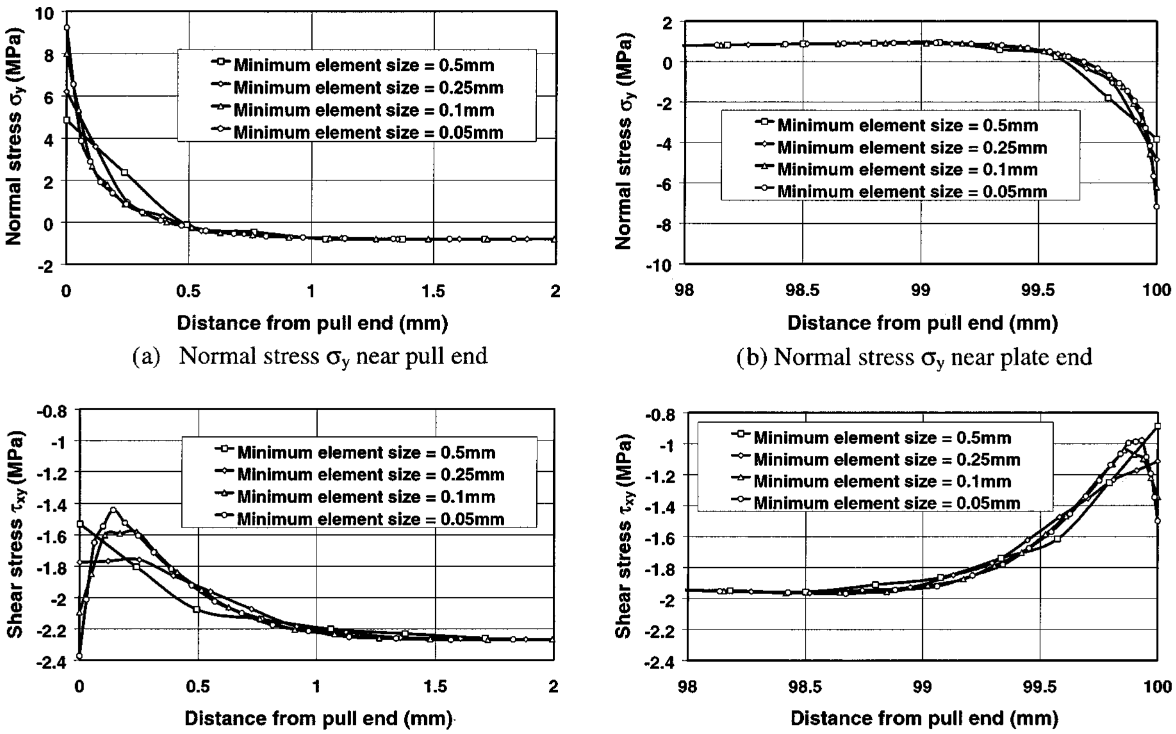

(a) Normal stress σ_y near pull end

(b) Normal stress σ_y near plate end

(c) Shear stress τ_{xy} near pull end

(d) Shear stress τ_{xy} near plate end

Fig. 5 Stresses on PA interface

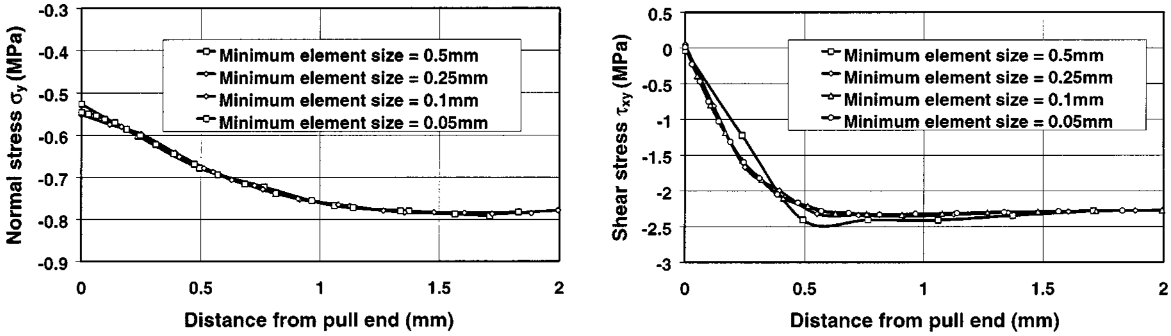

(a) Normal stress σ_y (b) Shear stress τ_{xy}

Fig. 6 Stresses in the adhesive at AM section near the pull end

stresses near the pull end have similar distribution and amplitude to those near the plate end (the sign is, however, reversed). A similar trend is seen for the shear stress distributions (Figs. 5c and d). They also show that the two coarse meshes failed to capture the descending part of the curves.

All four meshes predicted similar normal stress distributions at AM near the pull end (Fig. 6a). Except for the coarsest mesh, all other meshes predicted the same shear stress at AM (Fig. 6b). All predictions converged to zero shear stress at the free surface.

Although the stress will never converge because of stress singularities, differences between predictions using meshes with 0.1 and 0.05 mm smallest elements are only within 0.2 mm from the ends. Comparable meshes to that with 0.1 mm smallest elements were thus used for all other calculations hereafter. Fig. 7 shows the normal and shear stresses on PA, AM and AC over the whole bond length.

The shear stress in the concrete has maximum values near the adhesive/concrete interface, and it decreases gradually away from this interface (Fig. 8). Shear stress is believed to play a key role in the failure of shear test specimens. It can thus be expected that if a shear test specimen fails within the concrete it will be near the AC interface. This has been confirmed in many experiments (Chen and Teng 2001b).

Therefore, it would be ideal to investigate the stresses in the concrete near the AC interface. However,

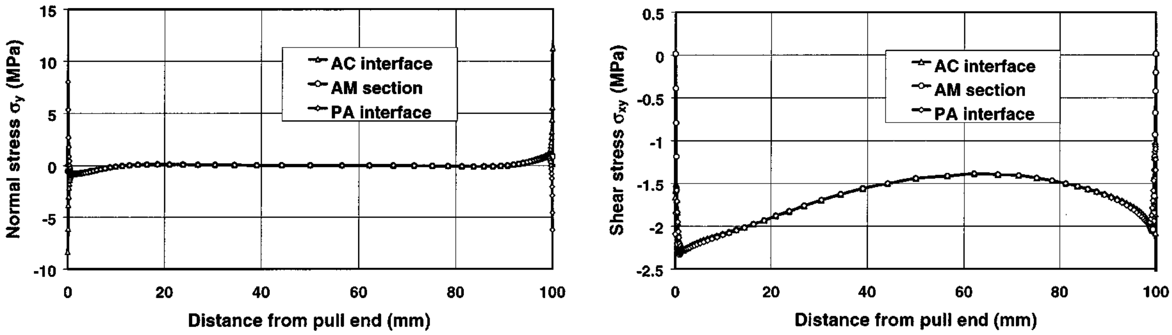

(a) Normal stress σ_y (b) Shear stres τ_{xy}

Fig. 7 Stresses in adhesive

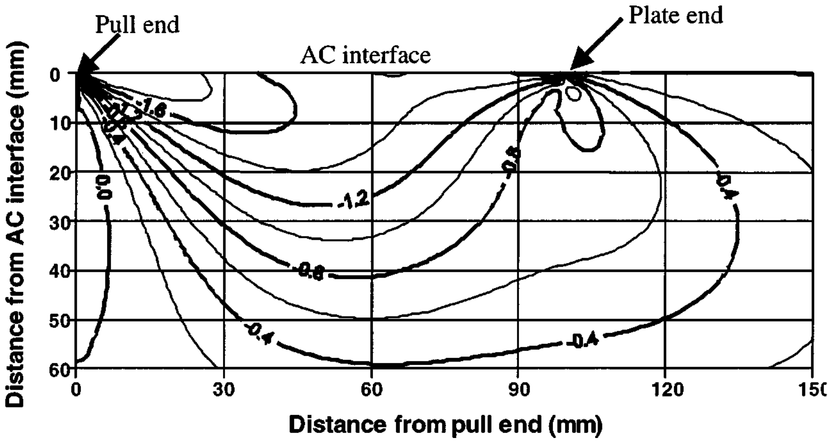

Fig. 8 Shear stesses in the concrete (MPa)

this is impractical because stress singularities at C and F (Fig. 4) mean that the stresses in the concrete at the AC interface near the pull and plate ends can not be accurately predicted. For this reason, the stresses at AM, which are much less sensitive to the mesh and are not singular, are used for comparison in the rest of this paper.

3.3. Stresses in the plate

Fig. 9 shows the distribution of the longitudinal stress on the upper and lower surfaces of the plate in a DoublePull test with a bond length $L = 100$ mm. Two boundary conditions were explored for the plate at the loading point: free or fixed vertically. When the loading point is free, the free part of the plate is subjected to pure tension. Within the bonded part of the plate, there are significant bending stresses near the pull end, with the stress on the upper surface about 30% larger than that on the lower surface at about 10 mm from the pull end. The bending effect decreases gradually as distance from the pull end x

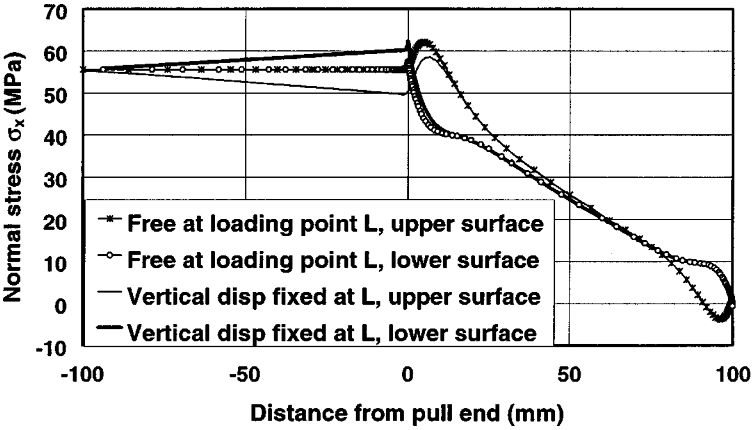

Fig. 9 Horizontal normal stress σ_x in the plate for double shear pulling test

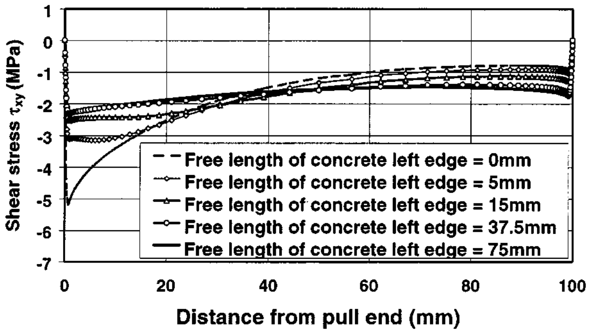

(a) Shear stress

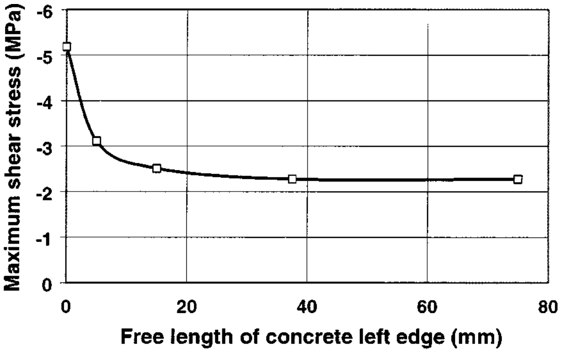

(b) Maximum shear stress near pull end

Fig. 10 Effect of support at the left edge of the concrete on shear stress at AM

(Fig. 3a) increases and becomes insignificant at about $x = 40$ mm. Near the plate end, the bending effect becomes significant again though the average stress approaches zero. The stress is larger on the lower surface than that on the upper surface here.

When the loading point is fixed vertically, the bending of the plate near the pulling end leads to reaction force at the constraint results in linearly increasing plate bending stresses from the loading point to the pulling end within the free part of the plate. The distributions of bending stresses within the bonded part of the plate are almost identical to those with a free loading point, except they are slightly smaller within $x < 20$ mm.

The interfacial shear stress at PA is usually found from the difference between adjacent two strains, measured on the upper surface along the bonded part of the plate in experimental studies (e.g., Swamy *et al.* 1986). This method is accurate only when the plate is subjected to pure tension within the bonded part. The existence of significant bending stresses within the plate means that the method can lead to significant errors, especially near the pull end.

These results show that the two boundary conditions at the loading point result in similar stress distributions within the bonded part of the plate, excepting small differences within $x < 20$ mm. Results show that this statement also stands for stresses at AP, AC and AM. In all following analyses, the loading point was fixed (which may be closer to practical conditions).

3.4. Boundary conditions for double shear pushing test

In double or single shear pushing tests (Figs. 1b and 1d), the pushing force on the concrete block is usually the reaction force at the supporting wedge or plate. The plate is usually very thick so it was modelled as a stiff support here. The effect of the plate size, which naturally varies in practical tests, was investigated here. Only the DoublePush test was modelled here, but the results shall also apply to the single shear-pushing test.

Five boundary conditions at the left edge of the concrete block were used. They are identified with the length of the free edge near the pull end (the rest of the left edge was constrained horizontally). These lengths were 0, 5, 15, 37.5 and 75 mm respectively for the five cases, corresponding to that the full, 14/15, 4/5, 1/2 and only the mid-height point of the left edge were horizontally constrained respectively. Fig. 10a shows the shear stress distribution on AM. When the free edge is greater than 37.5 mm, the size of the support has little effect. When it is reduced to 15mm, the shear stress is up to

25% larger near the pull end and up to 25% smaller near the plate end compared with only one mid-height point support. When the whole concrete edge is constrained, the shear stress is up to 100% larger than that with only one point constraint.

Fig. 10b shows that the maximum shear stress near the pull end decreases very fast when the length of free concrete edge increases if this length is small (<15 mm). The shear stresses in the adhesive, which transfer the load in the plate to the concrete, clearly play a key role in the failure of such joints. Although it is difficult to quantitatively relate the linear elastic predictions here to the bond strength (failure load), it can be expected that a large support plate can result in a smaller bond strength. If the support plate has a similar size to the concrete cross-section, a few millimetres difference of the plate size may lead to significant differences between the test results.

Because the results are insensitive to the length of concrete free edge when it is greater than 37.5 mm, one half of the left concrete edge was constrained for DoublePush (Fig. 3c) and SinglePush (Fig. 3d) tests in the following analyses. However, it should be kept in mind that such predicted maximum shear stresses are the lower bound for these tests.

4. Effect of test methods

An extensive parametric study was carried out to compare the stress distributions in the five test set-ups. Comparison showed that the stress distribution has little difference between the double and single shear pushing tests and between the double and single shear pulling tests. Therefore, only the DoublePull, DoublePush and BeamTest scenarios are compared in the following discussion. Due to space limitation, only stresses at AM are compared.

There is little difference between the shear stress distributions for DoublePush and DoublePull tests when the bond length $L = 60$ mm (Fig. 11a). Shear stresses vary little within $x < 30$ mm for all the three methods and they gradually increase thereafter to reach peaks near the plate end. Compared with shear tests, shear stress in the BeamTest is slightly smaller in mid-parts of the adhesive length but larger near the plate end.

When L is increased to 100 mm (Fig. 11b), both DoublePush and DoublePull tests again predicted almost the same shear stress near the pull end. The shear stress decreases continuously from the pull end but starts to increase again at between $x = 70 - 90$ mm and peaks near the plate end in both shear test methods. The peak near the plate end is significantly larger in the pulling (than pushing) test, but it is smaller than that near the pull end in both tests. The shear stress in DoublePull is now smaller in the mid-parts of the adhesive length and larger near the plate end than that in DoublePush. In BeamTest, the shear stress decreases more quickly when $x < 40$ mm and increases more quickly when $x > 60$ mm than that in the shear tests. The peak near the plate end has a much higher value than in shear tests and it is still higher than that near the pull end. A similar trend exists when L increases to 150 mm (Fig. 11c) and 200 mm (Fig. 11d), except that the peak near the plate end disappears in DoublePush and its value is now smaller than that near the pull end in the other two tests. When L increases to 300 mm, the shear stress reduces to zero at about $x = 230$ mm and keeps at zero thereafter in the DoublePush test (Fig. 11e).

Fig. 11f shows the variation of the peak shear stresses near the pull and the plate ends with L. The peak stress near the pull end reduces slightly as L increases from 60 to 150 mm for all three tests. They remain almost unchanged when L further increases. The value in the BeamTest is slightly smaller than that in the shear tests. This value is the same in both shear tests, but it should be noted that the value in

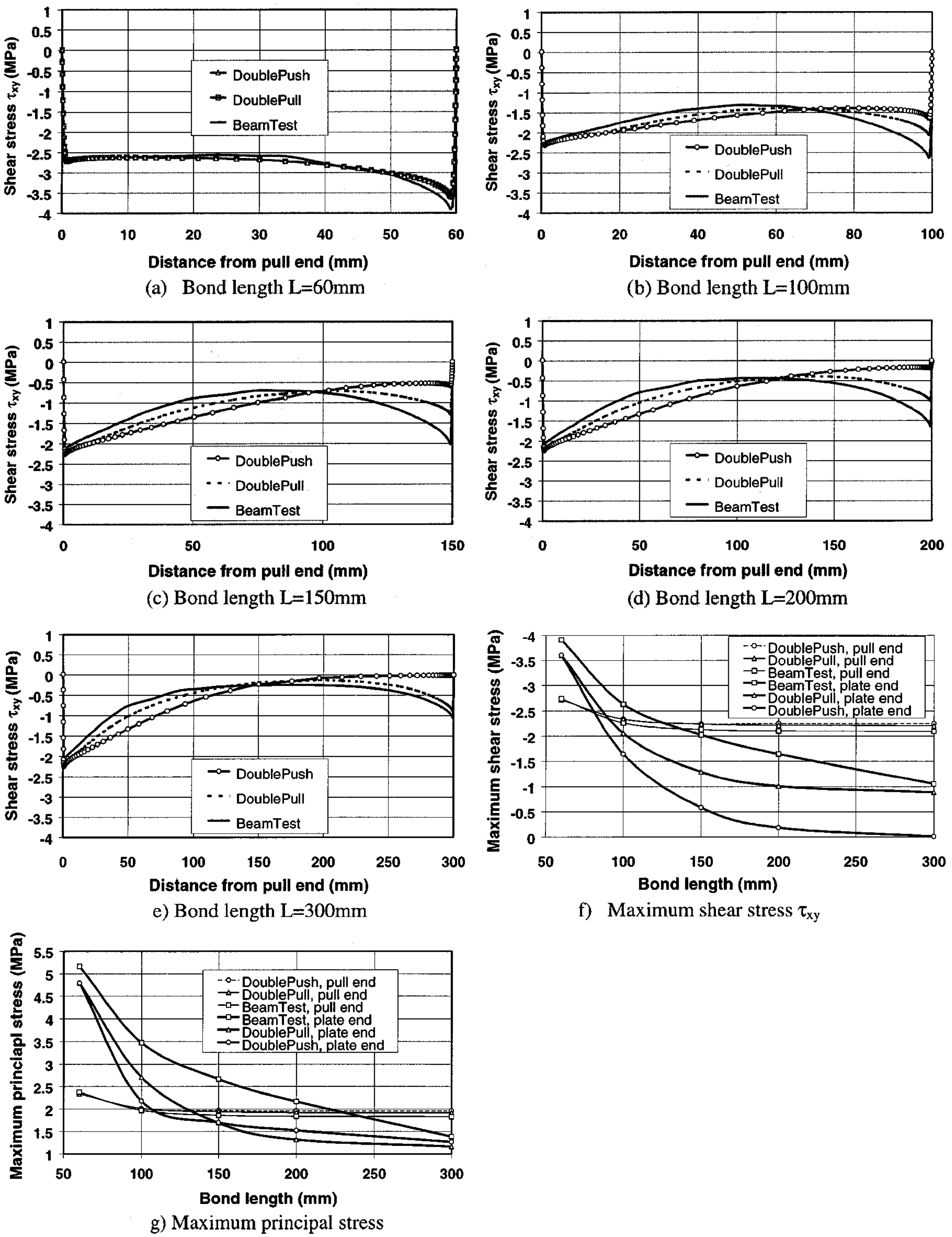

Fig. 11 Stresses at AM: various bond length

the pushing test is the lower bound due to the effect of the support plate size as discussed earlier. It may thus be expected that the bond strength would be lowest if obtained from shear pushing tests when the specimen fails from the pull end.

The peak shear stress near the plate end is higher than that near the pull end when L is small in all the three test methods. It reduces quickly as L increases and becomes smaller than that near the pull end. It decreases fastest in the DoublePush test and reaches zero when L is sufficiently large. This peak stress decreases slower in the DoublePull test and remains almost unchanged as L further increases from 200 mm to 300 mm. It decreases slowest in the BeamTest. The maximum major principal stress (Fig. 11g) shows a similar trend to the maximum shear stress, except that the maximum principal stress at the pull end exceeds that at the plate end at a longer bond length than the shear stress for all the three methods.

Fig. 12 shows the maximum stresses for various plate thickness with a constant bond length $L = 100$ mm. A constant tensile stress of $\sigma_x = 55.5$ MPa was applied at the plate end in all calculations. The maximum shear stress both near the pull and the plate ends increases as the plate thickness increases (Fig. 12a). The maximum shear stress near the plate end is smaller than that near the pull end when the plate thickness is small. It starts to exceed that near the pull end when the plate thickness is about 2.6, 3.4 and 4.4 mm for the BeamTest, DoublePull and DoublePush tests respectively. A similar trend exists for the maximum major principal stress (Fig. 12b), except that the maximum major principal stress near the plate end starts to exceed that near the pull end when the plate thickness increases to about 1.8, 2.4 and 2.9 mm for the BeamTest, DoublePull and DoublePush tests respectively.

If a constant load of 166.7 N/mm is applied instead of a constant stress, the maximum shear stress near the pull end decreases very quickly when the plate thickness t_p increases from 0.1 mm to 1 mm and then decreases more slowly when t_p further increases (Fig. 13a). The maximum shear stress near the plate end increases as t_p increases. The maximum principal stresses have the similar trends (Fig. 13b). These phenomena show that the applied load can be transferred to the concrete within a short bond length if the plate thickness is small and a longer bond length is required to transfer the same load if the plate is thick. This qualitatively confirms Chen and Tengs (2001b) bond strength model that the effective bond length increases as the plate thickness increases.

Based on above analysis, it can be expected that the failure of a specimen can start from either the plate end or the pull end. It is expected to start from the plate end if the bond length L is small or the

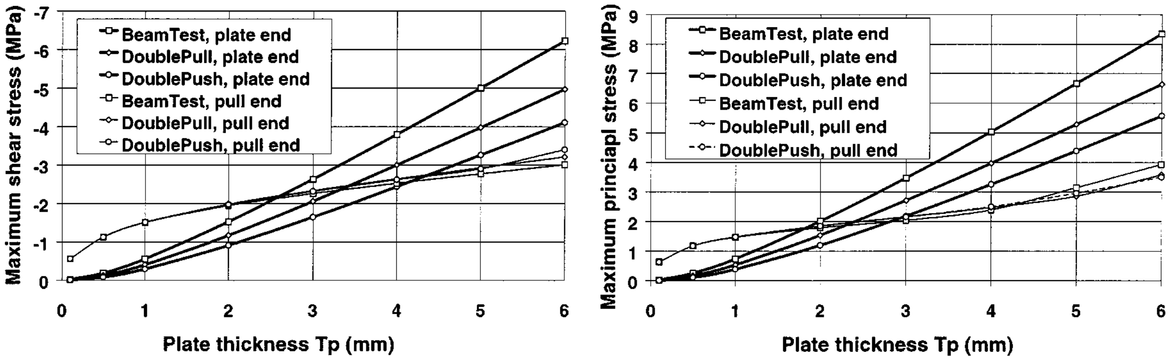

a) Maximum shear stress b) Maximum principal stress

Fig. 12 Effect of plate thickness on stresses at AM under constant plate stress

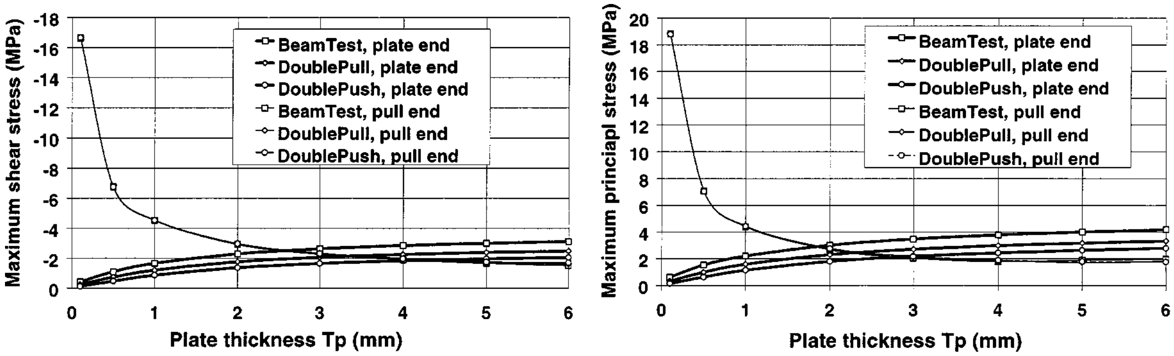

a) Maximum shear stress b) Maximum principal stress

Fig. 13 Effect of plate thickness on stresses at AM under constant plate load

plate thickness t_p is large, but start from the pull end if L is large or t_p is small. The values of L and t_p for the transition between these two failure modes are dependent on the adopted test method, with that the BeamTest has the largest L and smallest t_p, and that the DoublePush test the smallest L and largest t_p. Some other factors, which have not been studied here, are also expected to have significant effect on the stress distribution and thus the resultant test bond strength. These factors may include the thickness of the adhesive, and the Young's modulus of the adhesive, of the plate and of the concrete.

5. Conclusions

This paper has presented a review of experimental methods used for the FRP or steel plate to concrete bond strength test. Finite element analyses were carried out to study the stress distributions in different bond strength test methods. Based on the interpretation of numerical results, it is concluded that the size of support plate in shear pushing tests can have very significant effect on the tested bond strength if its size is close to the cross-sectional area of the concrete block.

Numerical results also indicate that two failure modes are possible: one starting from the plate end when the bond length is small and the plate is thick, and another starting from the pull end if the bond length is larger and the plate is thin. The transition values of bond length and plate thickness between these two failure modes are dependent on the adopted test method, with that in the bending test being largest for bond length and smallest for plate thickness, and in the shear pushing tests being smallest for bond length and largest for plate thickness.

The bond strength can be significantly dependent on the adopted test method. In general, the bond strength obtained using the bending test can be highest and that obtained using the shear pushing tests can be the lowest. Little difference can be expected between the double and single shear pushing tests, and between the double and single shear pulling tests.

References

Bizindavyi, L. and Neale, K.W. (1999), "Transfer lengths and bond strengths for composites bonded to concrete", *ASCE J. Comp. for Constr.*, **3**(4), 153-160.

Brosens, K. and Van Gemert, D. (1997), "Anchoring stresses between concrete and carbon fibre reinforced laminates", *Non-Metallic (FRP) Reinforced Concrete Structures, Proc., 3rd Int. Symp.*, 1, Oct., 271-278.

Chajes, M.J., Finch, W.W., Januszka, T.F. and Thonson, T.A. (1996), "Bond and force transfer of composite material plates bonded to concrete", *ACI Struct. J.*, **93**(2), 295-303.

Chen, J.F. and Teng, J.G. (2001a), "Shear capacity of FRP strengthened RC beams: FRP debonding", To be published.

Chen, J.F. and Teng, J.G. (2001b), "Anchorage strength models for FRP and steel plates bonded to concrete", accepted for publication by *ASCE J. Struct. Eng.*

Fukuzawa, K., Numao, T., Wu, Z., Yoshizawa, H. and Mitsui, M. (1997), "Critical strain energy release rate of interface debonding between carbon fibre sheet and mortar", *Non-Metallic (FRP) Reinforcement for Concrete Structures, Proc., 3rd Int. Symp.*, 1, Oct., 295-302.

Garden H.N. and Hollaway L.C. (1998), "An experimental study of the anchorage length of carbon fibre composite plates used to strengthen reinforced concrete beams", *Constr. Build. Mater.*, **12**(4), 203-219.

Hein, V.L. and Erdogan, F. (1971), "Stress singularities in a two-material wedge", *Int. J. Fracture Mech.*, **7**(3), 317-330.

Hiroyuki, Y. and Wu, Z. (1997), "Analysis of debonding fracture properties of CFS strengthened member subject to tension", *Non-Metallic (FRP) Reinforcement for Concrete Structures, Proc., 3rd Int. Symp.*, 1, Oct., 287-294.

Horiguchi, T. and Saeki, N. (1997), "Effect of test methods and quality of concrete on bond strength of CFRP sheet", *Non-metallic (FRP) Reinforcement for Concrete Structures, Proc., 3rd Int. Symp.*, 1, 265-270.

Jones, R., Swamy, R.N., Bloxham, J. and Bouderbalah, A. (1980), "Composite behaviour of concrete beams with epoxy bonded external reinforcement", *Int. J. Cement Compos.*, 2, 91-107.

Kobatake, Y., Kimura, K. and Ktsumata, H. (1993), "A retrofitting method for reinforced concrete structures using carbon fibre", *Fibre-Reinforced-Plastic (FRP) Reinforcement for Concrete Structures: Properties and Applications*, Elsevier Science Publishers, 435-450.

Maeda, T., Asano, Y., Sato, Y., Ueda, T. and Kakuta, Y. (1997), "A study on bond mechanism of carbon fiber sheet", *Non-Metallic (FRP) Reinforcement for Concrete Structures, Proc. 3rd Int. Symp.*, 1, 279-285.

Neubauer, U. and Rostásy, F.S. (1997), "Design aspects of concrete structures strengthened with externally bonded CFRP plates", *Proc., 7th Int. Conf. on Structural Faults and Repairs*, ECS Publications, Edinburgh, 2, 109-118.

Smith, S.T., Teng, J.G. and Chen, J.F. (2001), "Debonding in FRP plated RC beams induced by intermediate cracking", *Proc., ACUN-3 In. Comp. Conf.: Technology Convergence in Composites Applications*, 6-9 February, Sydney, Australia.

Swamy, R.N., Jones, R. and Charif, A. (1986), "Shear adhesion properties of epoxy resin adhesives", *Proc., Int. Symp. on Adhesion between Polymers and Concrete*, Sept., 741-755.

Täljsten, B. (1997), "Defining anchor lengths of steel and CFRP plates bonded to concrete", *Int. J. Adhes.*, **17**(4), 319-327.

Teng, J.G., Chen, J.F., Smith, S.T. and Lam, L. (2000), "RC structures strengthened with FRP composites", Hong Kong, China, 134 pp.

Teng, J.G., Zhang, J.W. and Smith, S.T. (2001), "Interfacial stresses in RC beams bonded with a soffit plate: a finite element study", to be published.

Van Gemert, D. (1980), "Force transfer in Epoxy-bonded steel-concrete joints", *Int. J. Adhes. Adhes.*, No. 1, 67-72.

Ziraba, Y.N., Baluch, M.H., Basunbul, A.M., Azad, A.K., Al-Sulaimani, G.J. and Sharif, I.A. (1995), "Combined experimental numerical approach to characterisation of steel-glue-concrete interface", *Mater. Struct.*, **28**, 518-525.

SC